

1 **Microstructure predicts non-motor outcomes following Deep**

2 **Brain Stimulation in Parkinson's disease**

3 Philipp A. Loehrer^{1*}, Miriam H. A. Bopp^{2,3}, Haidar S. Dafsari⁴, Sieglinde Seltenreich¹,

4 Susanne Knake^{1,3,5}, Christopher Nimsky^{2,3}, Lars Timmermann^{1,3,5}, David J. Pedrosa^{1,3#},

5 Marcus Belke^{1,5#}

6
7 ¹*Department of Neurology, Philipps-University Marburg, Marburg, Germany*

8 ²*Department of Neurosurgery, Philipps-University Marburg, Marburg, Germany*

9 ³*Center for Mind, Brain and Behavior (CMBB), Marburg, Germany*

10 ⁴*Department of Neurology, University Hospital Cologne, Cologne, Germany*

11 ⁵*Center for Personalized Translational Epilepsy Research (CePTER) Consortium*

12
13 *Corresponding author:

14 Philipp Loehrer, Department of Neurology, Philipps-University Marburg, Baldinger Str.,
15 35043, Marburg, Germany, Tel: +49 6421 5866419, Email: Loehrer@staff.uni-marburg.de

16 #Contributed equally

17
18 **Number of words in the abstract:** 213/250

19 **Number of words in the manuscript:** 3447/3500

20 **Number of tables and figures:** 3/8

21 **Number of References:** 40/40

22 **Character count title:** 98

23 **Key words:** non-motor symptoms, Parkinson's disease, deep brain stimulation, diffusion
24 imaging, NODDI, microstructure

1 **Abstract**

2 **Background:** Deep brain stimulation of the subthalamic nucleus (STN-DBS) is an effective
3 treatment for motor and non-motor symptoms in advanced Parkinson's disease (PD).
4 However, considerable interindividual variability of outcomes exists. Neuroimaging based
5 biomarkers, such as neurite orientation dispersion and density imaging (NODDI), a
6 biophysical model based MRI-technique, have been proposed to predict clinical outcomes and
7 therefore inform preoperative patient counselling.

8 **Objective:** To detect microstructural properties of brain areas associated with short-term non-
9 motor outcomes following STN-DBS in PD.

10 **Methods:** In this prospective open-label study, 37 PD patients underwent diffusion MRI and
11 comprehensive clinical assessments at preoperative baseline and 6-month follow-up. Neurite
12 density index (NDI), orientation dispersion index (ODI), and fractional anisotropy (FA) were
13 derived. Whole brain voxel-wise analysis assessed associations between microstructural
14 metrics and non-motor outcomes corrected for multiple comparisons using a permutation-
15 based approach.

16 **Results:** Intact microstructure within specific areas including right insular cortex, right
17 putamen, right cingulum, and bilateral corticospinal tract were associated with greater
18 postoperative improvement of non-motor symptom burden. Furthermore, microstructural
19 properties of distinct brain regions were associated with postoperative changes in sleep,
20 attention/memory, and urinary symptoms.

21 **Conclusion:** Microstructural properties of distinct brain areas predict non-motor outcomes in
22 DBS for PD. Therefore, diffusion MRI can support preoperative patient counselling and
23 treatment selection by identifying patients with above- or below-average non-motor
24 responses.

25

1 **Introduction**

2 Deep brain stimulation (DBS) of the subthalamic nucleus (STN) is an established therapy for
3 advanced Parkinson's disease (PD), improving motor- and non-motor symptoms.¹⁻³ Despite
4 significant therapeutic benefits at the group level, there is large variability in outcomes at the
5 individual subject-level, with some patients even experiencing persistent symptoms.⁴ To
6 predict postoperative outcomes and thereby improve preoperative patient counselling, the use
7 of neuroimaging-based markers has been proposed.⁴ In this regard, quantitative MRI
8 techniques such as neurite orientation dispersion and density imaging (NODDI) have gained
9 increasing attention in recent years to track disease progression and treatment response.⁵
10 NODDI is a multi-compartmental diffusion-weighted MRI technique which facilitates the
11 assessment of specific microstructural properties directly related to neurite morphology.⁶ The
12 model provides two voxelwise metrics of neurite morphology: the neurite density index
13 (NDI), describing the density of axons and dendrites within a voxel, and the neurite
14 orientation dispersion index (ODI), characterizing the variability of neurite orientations, i.e.
15 how parallel they are. Importantly, the relationship between NODDI metrics and underlying
16 tissue properties has recently been confirmed histologically.⁷ Despite its sensitivity and
17 specificity, NODDI protocols have a clinically feasible data acquisition time, making them an
18 important tool for use in clinical research.⁶ Previous studies employing NODDI in PD have
19 shown that the model is capable of differentiating PD patients from healthy controls¹¹ and
20 patients with atypical Parkinsonism.¹² Furthermore, NODDI characterized disease related
21 pathology such as retrograde degeneration of the nigrostriatal pathway,¹³ and its metrics were
22 associated with bimanual motor control,¹⁴ disease severity, and duration.^{6,11} Combining
23 NODDI with conventional DTI metrics in a multi-parametric analysis therefore provides
24 complementary information on microstructural properties and may serve as an imaging-based
25 marker to facilitate treatment prediction and inform patient counselling. Thus, we sought to

1 demonstrate that a multi-parametric quantitative MRI approach can detect microstructural
2 properties of brain areas that predict non-motor outcomes following STN-DBS in PD.
3 Specifically, we aimed to identify regions whose microstructural metrics, i.e. NDI, ODI, and
4 fractional anisotropy (FA), were associated with (1) changes in overall non-motor symptom
5 burden and (2) changes in non-motor symptom domains, showing significant improvements
6 after STN-DBS. The results of the present study should help to guide preoperative patient
7 counselling by identifying microstructure that predicts above- or below-average non-motor
8 response to STN-DBS.

9 **Methods**

10 The study was approved by the local ethics committee (study-number: 155/17) and carried out
11 in accordance with the Declaration of Helsinki.

12 **Participants.**

13 Thirty-seven PD patients (9 female, mean age 58.8 ± 7.3 years) were enrolled in this
14 prospective, observational, ongoing study upon written informed consent (for demographics
15 cf. Table 1). Inclusion criteria comprised indication for DBS lead surgery because of
16 advanced PD according to modern criteria.⁸ Patients were excluded if they had pathological
17 MR imaging, a concomitant neurological or psychiatric disease, or impaired visual or auditory
18 function.

1 **Clinical Assessment**

2 Patients were assessed preoperatively and six months after DBS lead surgery, with medication
3 at both times and DBS switched on postoperatively. All subjects underwent a
4 neuropsychological assessment including the Non-Motor Symptom Scale (NMSS), the
5 Parkinson's Disease Questionnaire (PDQ)-8 and the Scales for Outcomes in PD - Motor
6 Function (SCOPA-M) using standardized case report forms. Detailed information on the
7 clinical assessment is provided in the supplementary material.

8 **MRI Data Acquisition and Processing**

9 PD patients were scanned at baseline on a 3-Tesla Trio scanner (Siemens, Erlangen,
10 Germany) at the Core Unit Brain Imaging of the University of Marburg. The acquisition
11 protocol is reported in the supplementary material. All images were investigated to be free of
12 motion or ghosting and high frequency and/or wrap-around artefacts at the time of image
13 acquisition.

14 **Image Processing**

15 Image analysis was performed within the FreeSurfer image analysis suite 7.1.1
16 (<http://surfer.nmr.mgh.harvard.edu>) as reported previously by our group.⁹ The processing of
17 T1-weighted scans included skull stripping, automated Talairach transformation, cortical and
18 subcortical segmentation, intensity normalisation, tessellation of the grey/white matter
19 boundary, automated topology correction, and surface deformation following intensity
20 gradients.¹⁰

21 DTI data were processed using FMRIB Software Library (FSL) 6.0.5.2
22 (<https://fsl.fmrib.ox.ac.uk/fsl>). To correct for eddy-current distortions and involuntary
23 movements, raw DTI volumes were linearly registered and resampled to the first b0 volume.¹¹
24 Subsequently, the diffusion tensor for each voxel was fit to the data using linear regression
25 and FA was derived from the diffusion tensor.¹² Furthermore, NODDI-DTI,¹³ a modification

1 of NODDI,⁶ was used to obtain NDI and ODI from the DTI data. Visual inspection of the
2 b0-images confirmed that no changes beyond those in the tissue structure contributed to the
3 observed effects. To perform regional analyses, the first b0 image of each scan was linearly
4 registered to the structural T1-weighted image using a boundary based method, yielding an
5 affine matrix.¹⁴ Subsequently, T1-derived segmentations and brain masks were transformed to
6 the diffusion space via the inverse of the affine matrix.

7 **Statistical analysis**

8 Statistical analysis of clinical outcomes was performed in MATLAB (The MathWorks, Inc.,
9 R2018a). Changes between baseline and follow-up were analysed using the Wilcoxon signed-
10 rank or t-test when parametric test criteria were met. The type-I error was controlled using the
11 Benjamini-Hochberg method and effect sizes were calculated according to Cohen.
12 Relationships between change scores of clinical data and NMSS total score (NMSS-T) were
13 explored using Spearman correlations as reported previously.^{15,16}

14 Statistical voxelwise analysis of image data was performed using a generalized linear model.
15 First, FA-maps were co-registered to the MNI152 space using linear and nonlinear
16 transformation.¹⁷ Masked FA-, NDI-, and ODI-maps were subsequently registered to the
17 MNI152 space using the transformation from the previous step. Only voxels of brain tissue
18 existing in every subject were included in the analysis. Significant associations between
19 metrics of microstructure and change of non-motor symptoms were carried out for the whole
20 brain as described previously.¹⁸ Here, percentage differences between baseline and follow-up
21 values were calculated for NMSS-T and NMSS domains with significant postoperative
22 improvement ((2) sleep/fatigue, (5) attention/memory, and (7) urinary). A permutation-based
23 approach based on the Analysis of Functional NeuroImages (AFNI) null-z simulator was used
24 to corrected for multiple comparisons employing 12,000 simulations under the null
25 hypothesis.¹⁹ Clusters were formed using a threshold of $p < .01$ and a clusterwise p-value was
26 calculated. Results were accepted as significant with clusterwise $p < .05$.

1 **Results**

2 **Clinical outcomes**

3 Longitudinal changes of clinical outcomes are reported in Table 1. At the 6-month follow-up,
4 we observed improvements of NMSS-T ($z=-2.95$, $p=.007$, $r=-.34$), PDQ-8 SI ($t(36)=4.22$,
5 $p<.001$, Cohen's $d: .67$), and SCOPA-M total score ($z=-4.01$, $p<.001$, $r=-.47$), as well as
6 reductions of LEDD ($t(36)=7.63$, $p<.001$, Cohen's $d: 1.2$) and LEDD-DA ($t(36)=4.98$,
7 $p<.001$, Cohen's $d: .7$). Analysis of NMSS domains revealed beneficial effects of STN DBS
8 on sleep/fatigue (domain 2; $z=-3.79$, $p<.001$, $r=-.44$), attention/memory (domain 5; $z=-2.49$,
9 $p=.022$, $r=-.29$), and urinary symptoms (domain 7; $z=-2.39$, $p=.026$, $r=-.28$). Analysis of
10 SCOPA-M domains showed improvements in motor examination ($z=-2.87$, $p=.008$, $r=-.33$),
11 activities of daily living ($z=-3.27$, $p=.003$, $r=-.38$), and motor complications ($z=-3.76$, $p<.001$,
12 $r=-.44$) at the 6-month follow-up. Results of the correlation analysis are reported in the
13 supplementary materials (Table e-1).

14 **Interaction between Fractional Anisotropy and postoperative non-motor** 15 **symptom change**

16 Higher FA-values in the right insular cortex were associated with greater postoperative
17 NMSS-T reduction (positive cluster P1, cluster wise p-value (CWP): .032). Furthermore,
18 lower FA values were found in clusters including the bilateral cingulum and the left inferior
19 longitudinal fasciculus (ILF), which were related to greater postoperative NMSS-T reduction
20 (negative clusters N1-3, CWP: $<.001-.014$). Regional mean fractional anisotropy values
21 associated with postoperative change in non-motor symptom burden are detailed in Table e-2
22 and Figures e-1 and e-2.

1 **Interaction between NODDI-parameters and postoperative non-motor symptom**
2 **change**

3 Whole brain analysis of NODDI parameters showed that both, ODI and NDI, were associated
4 with changes in postoperative NMSS-T. Higher ODI-values in the right putamen, the right
5 cingulate cortex, and the left forceps major were related to a higher postoperative NMSS-T
6 reduction (P1-4, CWP: <.001-.034, Figure 1, Table e-3). Furthermore, lower ODI-values in
7 regions of both corticospinal tracts as well as left occipital fusiform gyrus were related to a
8 higher postoperative NMSS-T reduction (N1-4, CWP: <.001-.047, Figure 2, Table e-3).
9 Lower NDI-values in the left postcentral gyrus, left cingulum, and right forceps minor were
10 associated with a higher postoperative NMSS-T reduction (N1-4, CWP: <.001-.047, Figure e-
11 4, Table e-4). No positive associations between NDI-values and postoperative NMSS-T
12 change were detected.

13 **Interaction between microstructure and postoperative change in Non-Motor**
14 **Symptoms Scale domains**

15 Regional mean values of microstructural metrics associated with significant postoperative
16 changes in non-motor symptoms scale domains are detailed in Table e-5 (sleep/fatigue), Table
17 e-6 (attention/memory), and Table e-7 (urinary symptoms). Higher values of microstructural
18 metrics within vast regions of bilateral corticospinal tract (CST) were related to a higher
19 symptom reduction in the sleep and fatigue domain (FA: P1-2, CWP: .001-.005; ODI: P1-4,
20 CWP: <.001; NDI: P1, CWP: .004; Table e-5). With regard to attention and memory, higher
21 FA-values in bilateral cingulum, left insular cortex, and left anterior thalamic radiation
22 (AThR) were associated with higher postoperative symptom reduction (P1-4, CWP: <.001-
23 .031, Table e-6). Furthermore, higher ODI-values in left parahippocampal gyrus and within
24 the right frontal pole were related to positive postoperative outcomes in attention and memory
25 (P1-2, CWP: <.001-.049), whereas lower ODI-values in bilateral AThR and left cingulum

1 were associated with higher symptom reduction (N3, N5, N8-10, CWP: <.001-.039). Also,
2 vast areas of bilateral CST and putamen that had lower ODI- and NDI-values were associated
3 with higher symptom reduction in the attention/memory domain (ODI: N1, N2, N4 and N7-8,
4 CWP: <.001-.011; NDI: N1-6 CWP: <.001-.023). Concerning urinary symptoms, higher ODI-
5 and NDI-values in left putamen, pallidum, and AThR as well as left cerebellar lobule V and
6 VI were related to higher postoperative symptom reduction in the urinary domain (ODI: P1-3,
7 CWP: <.001-.031; NDI: P1-2, P4, CWP: <.001-.002, Table e-7). This association was also
8 present between NDI-values and right pallidum and putamen (P3, CWP: .002). Furthermore,
9 higher FA-values in right cingulate gyrus and left superior longitudinal fasciculus (SLF) were
10 associated with higher postoperative reduction of urinary symptoms (P1-2, CWP: <.001-.01).

11 **Discussion**

12 In the present study, NODDI-DTI, a novel method for analysing DWI data, was applied to
13 preoperative imaging to investigate cerebral microstructure associated with non-motor
14 symptom changes following neurostimulation in PD. There are two key findings. First, we
15 demonstrate that intact microstructure within specific areas including right insular cortex,
16 right putamen, right cingulum, and bilateral CST were associated with higher reduction of
17 postoperative non-motor symptom burden. Second, we delineate the structures and their
18 microstructural properties which are associated with postoperative improvements in specific
19 non-motor domains.

20 Whole brain analysis of NODDI parameters identified an association between higher ODI in
21 right putamen as well as right cingulum and a higher reduction of postoperative non-motor
22 symptom burden. As ODI is high in gray matter,⁶ this finding supports the notion that intact
23 sprawling of dendritic processes in these areas is important for beneficial postoperative non-
24 motor outcomes. In PD, the pathological deposition of alpha-synuclein in intraneuronal Lewy
25 inclusions is accompanied by a degeneration of neurons and severe morphological changes of

1 dendrites.^{20,21} These tissue changes cannot be seen in conventional MRI, whereas NODDI is
2 sensitive to neurite morphology.⁶ Indeed, previous work demonstrated reduced putaminal
3 ODI-values in patients with PD compared to healthy controls.²¹ This finding was interpreted
4 as decreased dendrite length and loss of spines of striatal medium spiny neurons, which are
5 the primary target of dopaminergic nigrostriatal projections.²¹ Considering the close
6 topographical relationship between STN and putamen as well as insular cortex and the
7 integration of STN in basal ganglia-thalamo-cortical loops with its motor, associative, and
8 limbic projections, it is important to examine the assumed mechanisms of action of DBS.^{4,22}
9 Besides effects on the micro- and mesoscale, the high-frequency pulses of electrical current
10 emitted by DBS electrodes affect interregional networks on the macroscale.⁴ Here,
11 modulation of networks has been able to predict postoperative outcomes across several motor
12 and non-motor symptoms.⁴ Furthermore, previous work has shown that compromised
13 putaminal microstructure in PD patients can be associated with higher non-motor symptom
14 burden independent of motor symptoms.²³ Therefore, it can be hypothesised that the positive
15 association between ODI and postoperative non-motor outcomes in the present study
16 represents the dependency of DBS on intact tissue structure to exert its network effects.
17 Besides associations with gray matter areas, ODI showed a negative association with
18 postoperative non-motor symptom burden in bilateral CST. In healthy white matter tissue,
19 ODI is usually low, as fibers are highly coherent to another whereby high values of ODI
20 represent axonal disorganisation and degeneration.⁶ Therefore, the observed negative
21 association might reflect the dependence of DBS on intact tissue structure in CST, as low
22 ODI, i.e. intact white matter microstructure, was associated with beneficial postoperative
23 outcomes. Previous DTI-studies have repeatedly demonstrated microstructural alterations of
24 CST in PD. In particular, increased FA has consistently been reported and hypothesised to
25 demonstrate a compensatory mechanism, reflecting axonal sprouting secondary to a reduced
26 input from striatum and thalamus.²⁴ When, however, microstructure in CST deteriorates over

1 the course of the disease, an association with motor dysfunction was demonstrated.²⁵
2 Associations between altered CST-microstructure and non-motor symptoms, on the other
3 hand, have received little attention. Employing a connectometry analysis in 85 patients,
4 Ashraf-Ganjouei and colleagues could demonstrate that lower axonal density in CST was
5 associated with a higher burden of gastrointestinal symptoms.²⁶ Furthermore, lower FA-
6 values in right CST were observed in PD patients with depression compared to non-depressed
7 patients.²⁷ Extending these findings, the results of the present study demonstrate that not only
8 non-motor symptoms but also beneficial non-motor outcomes following STN-DBS depend on
9 intact CST microstructure. Considering the role of the CST as major effector of motor control,
10 motor outcomes and the postoperative reduction in dopaminergic medication could contribute
11 to the beneficial non-motor effects in the present study. Importantly, however, postoperative
12 improvements in non-motor symptom burden were not related to improvements in LEDD,
13 LEDD-DA, and SCOPA-motor examination scores, which is in accordance with the
14 literature.^{28,29} Therefore, the association between intact CST microstructure and beneficial
15 postoperative non-motor outcomes seems to be independent of the motor effects of DBS and
16 suggests that CST microstructure is inherently relevant for non-motor symptoms in PD.

17 **Microstructure is associated with beneficial sleep outcomes**

18 Sleep disturbances affect the majority of PD patients and result in poor quality of life.³⁰
19 Associated disorders encompass both, disturbances of sleep-wake transition, as well as
20 parasomnias.³⁰ Although the exact neural mechanisms remain to be established, a disrupted
21 interaction of neuronal circuits and different neurotransmitter systems has been suggested to
22 underlie the sleep disturbances in PD.^{31,32} STN-DBS has been suggested to improve sleep by
23 alleviating motor symptoms and directly altering sleep physiology resulting in increased total
24 sleep time, sleep efficiency, and quality of sleep as well as reduced wakefulness after sleep
25 onset and insomnia.³⁰ In the present study, STN-DBS improved symptoms of the sleep/fatigue
26 domain and beneficial outcomes were associated with higher FA-, ODI-, and NDI-values in

1 vast regions of the CST. On the other hand, lower ODI- and NDI-values in these areas were
2 associated with detrimental or below average response to STN-DBS. As most of the clusters
3 were overlapping and within regions of high fiber crossing and dispersion, the selective
4 degeneration of crossing fibers might underlie the observed relationship. The results,
5 therefore, support the hypothesis that intact microstructure of the CST and its crossing fibers
6 is important for beneficial postoperative changes in the sleep and fatigue domain.
7 Additionally, high ODI-values of cortical structures including right superior and middle
8 temporal gyrus and right parietal operculum cortex were associated with beneficial
9 postoperative outcomes. Previous studies of healthy controls using simultaneous recordings of
10 electroencephalography and functional MRI during sleep reported an association of activity
11 increases within these areas with sleep spindles during early stages of non-rapid eye
12 movement (NREM) sleep.³³ In PD, spindle density and amplitude seems to be reduced during
13 NREM and modulated by dopaminergic therapy.³⁰ Integrating these findings with results of
14 the present study one could speculate that intact microstructure, i.e. dendritic arborisation, in
15 these areas is important for STN-DBS to modulate sleep physiology.

16 **Microstructure is associated with beneficial attention and memory outcomes**

17 Higher FA (left hemisphere) and lower ODI in bilateral AThR were associated with beneficial
18 postoperative outcomes in the attention and memory domain. These results suggest, that
19 degenerative changes in axonal structure underlying FA alterations in AThR are attributable
20 to changes in axonal fanning and dispersion. AThR connects the frontal lobe, the dorsolateral
21 prefrontal cortex (DLPFC) in particular, with the anterior and midline nuclei of the
22 thalamus.²² As these nuclei are integrated in functional loops with the cingulum and the
23 pallidum, the nuclei and their fiber connections are associated with the limbic system and
24 thought to be involved in executive functions and planning of complex behaviour.^{22,34} The
25 DLPFC is involved in various higher-level cognitive functions including attention, working
26 memory, and executive control.^{35,36} Considering the functional association of AThR with

1 STN, as well as its role in connecting the structures named above, it seems reasonable that
2 intact microstructure in AThR is important for the conveyance of beneficial effects on
3 memory function and attention.

4 Higher FA and lower ODI in overlapping clusters in bilateral cingulum as well as associated
5 structures were related to increases in postoperative attention and memory function, indicating
6 that axonal fanning and dispersion underlies alterations in FA in the cingulum. The cingulum
7 is a group of nerve fibers connecting the hippocampus, prefrontal, parietal, and anterior
8 cingulate cortex.³⁷ This allows for the integration of information from these structures and
9 explains the involvement of the cingulum in attention, memory, and emotion regulation.³⁷
10 Previous studies in PD have shown that compromised microstructure of the cingulum was
11 related to reduced scores in cognitive assessments, impaired visuospatial memory, and
12 dementia.³⁸ Taken together, the association between microstructural properties and beneficial
13 attention and memory outcomes in bilateral AThR and cingulum might represent the
14 dependency of DBS on intact tissue structure to exert its network effects.

15 **Microstructure is associated with beneficial outcomes of urinary symptoms**

16 Deficient perception of multimodal sensory information is a characteristic of PD leading to
17 debilitating non-motor symptoms.³⁹ Sensory deficiencies in PD have been described in both,
18 somatosensory pathways associated with proprioception as well as visceral pathways involved
19 in monitoring of urinary bladder filling.⁴⁰ STN-DBS in PD was shown to improve the
20 perception of urinary bladder filling, resulting in a delayed desire to void and increased
21 bladder capacity.³⁹ Improved urinary function was attributed to a beneficial influence of STN-
22 DBS on a gain of afferent bladder information due to an increase or decrease of activation of
23 primary sensory areas.³⁹ In particular, previous studies showed an activation of anterior
24 cingulate gyrus (ACC) and left lateral frontal cortex during monitoring and controlling the
25 storage phase of the urinary cycle and these structures are thought to be involved in the urge
26 to void, withholding urine, and the onset of micturition.³⁹ In the present study, intact

1 microstructure, i.e. high FA, in right ACC was associated with postoperative improvements in
2 urinary symptoms suggesting that sound microstructure in ACC is necessary for STN-DBS to
3 have beneficial effects on controlling the storage phase of the urinary cycle. Furthermore,
4 high NDI and ODI, i.e. high dispersion without a decrease in axonal density, in left AThR
5 was associated with positive outcomes of urinary symptoms. AThR connects the frontal
6 cortex with the thalamus and the pallidum and previous studies suggested that modulation of
7 left frontal cortex by STN-DBS is important for urge control.³⁹ Therefore, intact
8 microstructure in left AThR might be relevant for STN-DBS to modulate left frontal cortex
9 during urge control.³⁹ Further important structures implicated in processing afferent urinary
10 bladder information are posterior thalamus, which is activated during bladder filling and
11 micturition, and ventrolateral as well as reticular thalamus, which receive input from the
12 striatum to modulate the flow of visceral information between posterior thalamus and the
13 cortex. Previous studies speculated that STN-DBS may recondition the interaction between
14 pallidal output and the modulatory effect of the thalamus, resulting in improved gating of
15 sensory information.³⁹ One might speculate, that the association of intact microstructure in
16 left pallidum and putamen with better outcomes in the urinary domain represents the
17 importance of these structures for the effect of STN-DBS on gating sensory information.

18 **Limitations**

19 Three main limitations of our study have to be addressed. First, despite histopathological
20 validation of the NODDI model and its frequent use in PD, no studies validating the model in
21 post-mortem brain tissue of PD patients exist. Second, the underlying assumptions of the
22 NODDI model may represent an oversimplification and might therefore result in reduced
23 specificity.⁶ Third, the resolution of the DTI scan is limited to 2.0x2.0x2.0mm, which might
24 be too coarse for valid assessments of small fiber bundles.

1 **Conclusion**

2 In conclusion, we describe a spatially distinct profile of microstructural alterations associated
3 with beneficial non-motor outcomes following neurostimulation in PD, including right insular
4 cortex, putamen, cingulum, and bilateral corticospinal tract. Furthermore, we delineate the
5 structures and their microstructural properties which are associated with postoperative
6 improvements in specific non-motor domains. Therefore, we suggest that diffusion MRI can
7 support preoperative patient counselling by identifying patients with above- or below-average
8 non-motor responses.

9 **Acknowledgement**

10 The authors would like to thank the participants for their active engagement in this study.

11 **Data and Code Availability**

12 The data that support the findings of this study are available on request from the
13 corresponding author (PAL). The data are not publicly available due to privacy or ethical
14 restrictions. All tools used for the analysis of MRI data are based on FreeSurfer Version 7.1
15 (<http://surfer.nmr.mgh.harvard.edu/>) and FSL 6.0.5.2 (<http://www.fmrib.ox.ac.uk/fsl>)
16 packages, which are freely available. Scripts for automation were written in tcshell and parts
17 of the statistics were written in Python using the packages numpy, pandas, seaborn,
18 matplotlib, nibabel and scipy, which are also freely available. Python program code for the
19 analysis of NODDI-DTI is available from <https://github.com/dicent/DTI-NODDI>.

20 **Contributorship**

21 PAL: study concept and design, data acquisition, data analysis, drafting of the manuscript

22 MBo: data acquisition, surgical intervention, critical revision of the manuscript

23 HSD: study design, critical revision of the manuscript

- 1 SS: data acquisition, critical revision of the manuscript
- 2 SK: critical revision of the manuscript
- 3 CN: data acquisition, surgical intervention, critical revision of the manuscript
- 4 LT: study design, critical revision of the manuscript
- 5 DJP: study concept and design, data acquisition, data analysis, drafting of the manuscript
- 6 MBe: study concept and design, data acquisition, data analysis, drafting of the manuscript

7 **Financial disclosure/Conflicts of Interest**

8 PAL was supported by the SUCCESS-Program of the Philipps-University of Marburg and the
9 ‘Stiftung zur Förderung junger Neurowissenschaftler’. MBo is a scientific consultant for
10 Brainlab. HSD was funded by the EU Joint Programme – Neurodegenerative Disease
11 Research (JPND), the Prof. Klaus Thiemann Foundation in the German Society of Neurology,
12 the Felgenhauer Foundation, the KoelnFortune program of the Medical Faculty of the
13 University of Cologne and has received honoraria by Everpharma, Kyowa Kirin, Bial, Oruen,
14 and Stadapharm. SS reports no financial disclosures. SK reports no financial disclosures. CN
15 is a scientific consultant for Brainlab. LT received payments as a consultant for Medtronic
16 Inc. and Boston Scientific and received honoraria as a speaker on symposia sponsored by
17 Bial, Zambon Pharma, UCB Schwarz Pharma, Desitin Pharma, Medtronic, Boston Scientific,
18 and Abbott. The institution of LT, not LT personally, received funding by the German
19 Research Foundation, the German Ministry of Education and Research, and Deutsche
20 Parkinson Vereinigung. DJP has received honoraria for speaking at symposia sponsored by
21 Boston Scientific Corp, Medtronic, AbbVie Inc, Zambon and Esteve Pharmaceuticals GmbH.
22 He has received honoraria as a consultant for Boston Scientific Corp and Bayer, and he has
23 received a grant from Boston Scientific Corp for a project entitled "Sensor-based optimisation
24 of Deep Brain Stimulation settings in Parkinson's disease" (COMPARE-DBS). The institution
25 of DJP, not DJP personally, has received funding from the German Research Foundation, the

1 German Ministry of Education and Research, the International Parkinson Foundation, the
2 Horizon 2020 programme of the EU Commission and the Pohl Foundation in Marburg.
3 Finally, DJP has received travel grants to attend congresses from Esteve Pharmaceuticals
4 GmbH and Boston Scientific Corp. MBe reports no financial disclosures.

5 **References**

- 6 1. Jost ST, Sauerbier A, Visser-Vandewalle V, et al. A prospective, controlled study of non-motor
7 effects of subthalamic stimulation in Parkinson's disease: results at the 36-month follow-up.
8 *Journal of neurology, neurosurgery, and psychiatry*. 2020;91(7):687-694.
- 9 2. Jost ST, Visser-Vandewalle V, Rizos A, et al. Non-motor predictors of 36-month quality of life
10 after subthalamic stimulation in Parkinson disease. *NPJ Parkinson's disease*. 2021;7(1):48.
- 11 3. Sauerbier A, Bachon P, Ambrosio L, et al. The New Satisfaction with Life and Treatment Scale
12 (SLTS-7) in Patients with Parkinson's Disease. *J Parkinsons Dis*. 2021.
- 13 4. Hollunder B, Rajamani N, Siddiqi SH, et al. Toward personalized medicine in connectomic
14 deep brain stimulation. *Prog Neurobiol*. 2022;210:102211.
- 15 5. Kamiya K, Hori M, Aoki S. NODDI in clinical research. *Journal of neuroscience methods*.
16 2020;346:108908.
- 17 6. Zhang H, Schneider T, Wheeler-Kingshott CA, Alexander DC. NODDI: Practical in vivo neurite
18 orientation dispersion and density imaging of the human brain. *NeuroImage*.
19 2012;61(4):1000-1016.
- 20 7. Grussu F, Schneider T, Tur C, et al. Neurite dispersion: a new marker of multiple sclerosis
21 spinal cord pathology? *Ann Clin Transl Neurol*. 2017;4(9):663-679.
- 22 8. Postuma RB, Berg D, Adler CH, et al. The new definition and diagnostic criteria of Parkinson's
23 disease. *The Lancet Neurology*. 2016;15(6):546-548.
- 24 9. Loehrer PA, Weber I, Oehr CR, et al. Microstructural alterations predict impaired bimanual
25 control in Parkinson's disease. *Brain communications*. 2022;4(3):fcac137.
- 26 10. Fischl B. FreeSurfer. *NeuroImage*. 2012;62(2):774-781.
- 27 11. Jenkinson M, Smith S. A global optimisation method for robust affine registration of brain
28 images. *Medical Image Analysis*. 2001;5:143-156.
- 29 12. Pierpaoli C, Basser PJ. Toward a quantitative assessment of diffusion anisotropy. *Magnetic
30 Resonance in Medicine*. 1996;36:893-906.
- 31 13. DTI-NODDI. Implementation of diffusion tensor image based neurite orientation dispersion
32 and density imaging (DTI-NODDI) written in Python. Available from
33 <https://github.com/dicemt/DTI-NODDI> [computer program]. <https://github.com/dicemt/DTI-NODDI2020>.
- 34 14. Greve DN, Fischl B. Accurate and robust brain image alignment using boundary-based
35 registration. *NeuroImage*. 2009;48:63-72.
- 36 15. Jost ST, Konitsioti A, Loehrer PA, et al. Non-motor effects of deep brain stimulation in
37 Parkinson's disease motor subtypes. *Parkinsonism Relat Disord*. 2023:105318.
- 38 16. Jost ST, Strobel L, Rizos A, et al. Gender gap in deep brain stimulation for Parkinson's disease.
39 *NPJ Parkinson's disease*. 2022;8(1):47.
- 40 17. Andersson JLR, Jenkinson M, Smith S. Non-linear registration, aka spatial normalisation. -
41 FMRIB technical report TR07JA2 from www.fmrib.ox.ac.uk/analysis/techrep. 2007.
- 42 18. Belke M, Unger M, Hattemer K, et al. Diffusion Tensor Imaging (DTI) in idiopathic REM sleep
43 behaviour disorder (iRBD). *Klinische Neurophysiologie*. 2010;41.
- 44

- 1 19. Nichols TE, Holmes AP. Nonparametric permutation tests for functional neuroimaging: A
2 primer with examples. *Human brain mapping*. 2002;15:1-25.
- 3 20. Halliday GM, Leverenz JB, Schneider JS, Adler CH. The neurobiological basis of cognitive
4 impairment in Parkinson's disease. *Movement disorders : official journal of the Movement
5 Disorder Society*. 2014;29(5):634-650.
- 6 21. Kamagata K, Hatano T, Okuzumi A, et al. Neurite orientation dispersion and density imaging
7 in the substantia nigra in idiopathic Parkinson disease. *European radiology*. 2016;26(8):2567-
8 2577.
- 9 22. Bähr M, Frotscher M. Neurologisch-topische Diagnostik Anatomie - Funktion - Klinik. 2014.
- 10 23. Lenfeldt N, Hansson W, Larsson A, Nyberg L, Birgander R, Forsgren L. Diffusion tensor
11 imaging and correlations to Parkinson rating scales. *Journal of Neurology*.
12 2013;260(11):2823-2830.
- 13 24. Atkinson-Clement C, Pinto S, Eusebio A, Coulon O. Diffusion tensor imaging in Parkinson's
14 disease: Review and meta-analysis. *NeuroImage: Clinical*. 2017;16:98-110.
- 15 25. Zhan W, Kang GA, Glass GA, et al. Regional alterations of brain microstructure in Parkinson's
16 disease using diffusion tensor imaging. *Movement Disorders*. 2012;27(1):90-97.
- 17 26. Ashraf-Ganjouei A, Majd A, Javinani A, Aarabi MH. Autonomic dysfunction and white matter
18 microstructural changes in drug-naïve patients with Parkinson's disease. *PeerJ*. 2018;6:e5539.
- 19 27. Ansari M, Adib Moradi S, Ghazi Sherbaf F, Hedayatnia A, Aarabi MH. Comparison of structural
20 connectivity in Parkinson's disease with depressive symptoms versus non-depressed: a
21 diffusion MRI connectometry study. *International psychogeriatrics*. 2019;31(1):5-12.
- 22 28. Petry-Schmelzer JN, Krause M, Dembek TA, et al. Non-motor outcomes depend on location
23 of neurostimulation in Parkinson's disease. *Brain : a journal of neurology*. 2019;142(11):3592-
24 3604.
- 25 29. Sauerbier A, Loehrer P, Jost ST, et al. Predictors of short-term impulsive and compulsive
26 behaviour after subthalamic stimulation in Parkinson disease. *Journal of neurology,
27 neurosurgery, and psychiatry*. 2021;92(12):1313-1318.
- 28 30. Zahed H, Zuzuarregui JRP, Gilron R, Denison T, Starr PA, Little S. The Neurophysiology of
29 Sleep in Parkinson's Disease. *Movement disorders : official journal of the Movement Disorder
30 Society*. 2021;36(7):1526-1542.
- 31 31. Qamar MA, Sauerbier A, Politis M, Carr H, Loehrer P, Chaudhuri KR. Presynaptic
32 dopaminergic terminal imaging and non-motor symptoms assessment of Parkinson's disease:
33 evidence for dopaminergic basis? *NPJ Parkinson's disease*. 2017;3:5.
- 34 32. Jost ST, Ray Chaudhuri K, Ashkan K, et al. Subthalamic Stimulation Improves Quality of Sleep
35 in Parkinson Disease: A 36-Month Controlled Study. *J Parkinsons Dis*. 2021;11:323-335.
- 36 33. Schabus M, Dang-Vu TT, Albouy G, et al. Hemodynamic cerebral correlates of sleep spindles
37 during human non-rapid eye movement sleep. *Proceedings of the National Academy of
38 Sciences*. 2007;104(32):13164-13169.
- 39 34. Nettersheim FS, Loehrer PA, Weber I, et al. Dopamine substitution alters effective
40 connectivity of cortical prefrontal, premotor, and motor regions during complex bimanual
41 finger movements in Parkinson's disease. *NeuroImage*. 2019;190:118-132.
- 42 35. Loehrer PA, Nettersheim FS, Jung F, et al. Ageing changes effective connectivity of motor
43 networks during bimanual finger coordination. *NeuroImage*. 2016;143:325-342.
- 44 36. Loehrer PA, Nettersheim FS, Oehrn CR, et al. Increased prefrontal top-down control in older
45 adults predicts motor performance and age-group association. *NeuroImage*.
46 2021;240:118383.
- 47 37. Wu Y, Sun D, Wang Y, Wang Y, Ou S. Segmentation of the Cingulum Bundle in the Human
48 Brain: A New Perspective Based on DSI Tractography and Fiber Dissection Study. *Front
49 Neuroanat*. 2016;10:84.
- 50 38. Chen B, Fan GG, Liu H, Wang S. Changes in anatomical and functional connectivity of
51 Parkinson's disease patients according to cognitive status. *European Journal of Radiology*.
52 2015;84(7):1318-1324.

- 1 39. Herzog J, Weiss PH, Assmus A, et al. Improved sensory gating of urinary bladder afferents in
2 Parkinson's disease following subthalamic stimulation. *Brain : a journal of neurology.*
3 2008;131(Pt 1):132-145.
- 4 40. Sakakibara R, Hattori T, Uchiyama T, Yamanishi T. Videourodynamic and sphincter motor unit
5 potential analyses in Parkinson's disease and multiple system atrophy. *Journal of neurology,*
6 *neurosurgery, and psychiatry.* 2001;71(5):600-606.

7
8
9
10
11
12
13
14
15
16
17
18
19
20
21
22

1 Tables

2 **Table 1: Baseline characteristics and outcomes at baseline and 6-month follow-up**

	<i>n</i>	<i>M</i>	<i>SD</i>					
Age [y]	37	58.8	7.3					
Disease duration [y]	37	8.9	4.3					
Sex (female/male) [%]	37	9/28	[24.3/75.7]					
	Baseline			6-MFU			Baseline vs. 6-MFU	
	<i>n</i>	<i>M</i>	<i>SD</i>	<i>n</i>	<i>M</i>	<i>SD</i>	<i>p</i>	<i>effect size</i>
NMSS total score	37	71.9	39.1	37	48.4	29.1	.007	-.34
Cardiovascular	37	1.6	2.7	37	1.1	2.5	.225	-.15
Sleep/fatigue	37	16.9	11.5	37	7.9	7.6	<.001	-.44
Mood/ apathy	37	11.6	13.3	37	6.0	7.6	.109	-.21
Perceptual problems/ hallucinations	37	.9	2.5	37	1.1	3.0	.865	-.03
Attention/ memory	37	7.0	6.5	37	5.0	5.9	.022	-.29
Gastrointestinal	37	5.6	5.0	37	4.4	4.9	.223	-.16
Urinary	37	13.2	10.4	37	9.1	10.2	.026	-.28
Sexual function	37	3.8	5.0	37	3.0	4.3	.296	-.13
Miscellaneous	37	11.2	8.9	37	10.7	7.8	.865	-.02
PDQ-8 SI	37	32.3	14.8	37	22.6	14.1	<.001	.67
SCOPA-M total score	37	19.8	6.2	37	12.9	6.4	<.001	-.47
SCOPA-M-motor examination	37	9.4	4.2	37	6.7	4.1	.008	-.33
SCOPA-M-activities of daily living	37	6.6	2.7	37	4.1	3.1	.003	-.38
SCOPA-M-motor complications	37	3.8	2.3	37	2.1	2.4	<.001	-.44
LEDD [mg]	37	962.3	393.2	37	537.6	269.0	<.001	1.2
LEDD DA [mg]	37	261.8	133.6	37	170.6	123.8	<.001	.7

1 **Table 1:** Demographic characteristics and outcome parameters at baseline and 6-months
2 follow-up. Reported p-values are corrected for multiple comparisons using Benjamini-
3 Hochberg’s method. Bold font highlights significant results, $p < .05$.

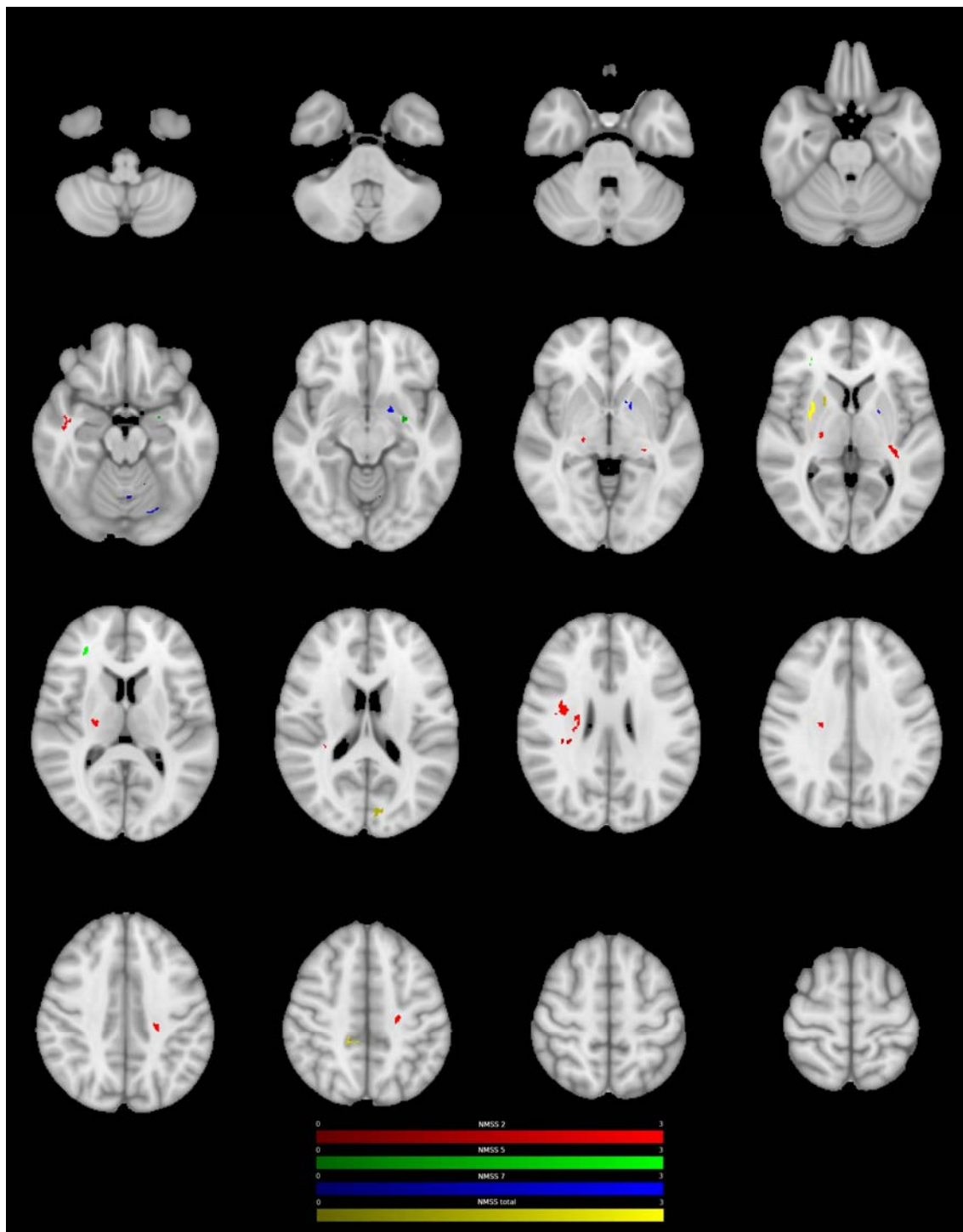
4 **Abbreviations:** 6-MFU = 6-month follow-up; LEDD = Levodopa equivalent daily dose;
5 LEDD-DA: LEDD of Dopamine Agonists; NMSS = Non-Motor Symptom Scale; PDQ-8 SI =
6 8-item Parkinson’s Disease Questionnaire summary index; SCOPA = Scales for Outcomes in
7 Parkinson’s disease;

8

9

10

1 Figures



3 **Figure 1.** Clusters with a positive association between PD patients' ODI-values and
4 postoperative change in NMSS-T (yellow), Domain 2 (sleep/fatigue, red), Domain 5
5 (attention/memory, green), and Domain 7 (urinary, blue), as revealed by the whole brain

1 analysis. P-Values were corrected for multiple comparisons using a permutation-based
2 approach.

3
4

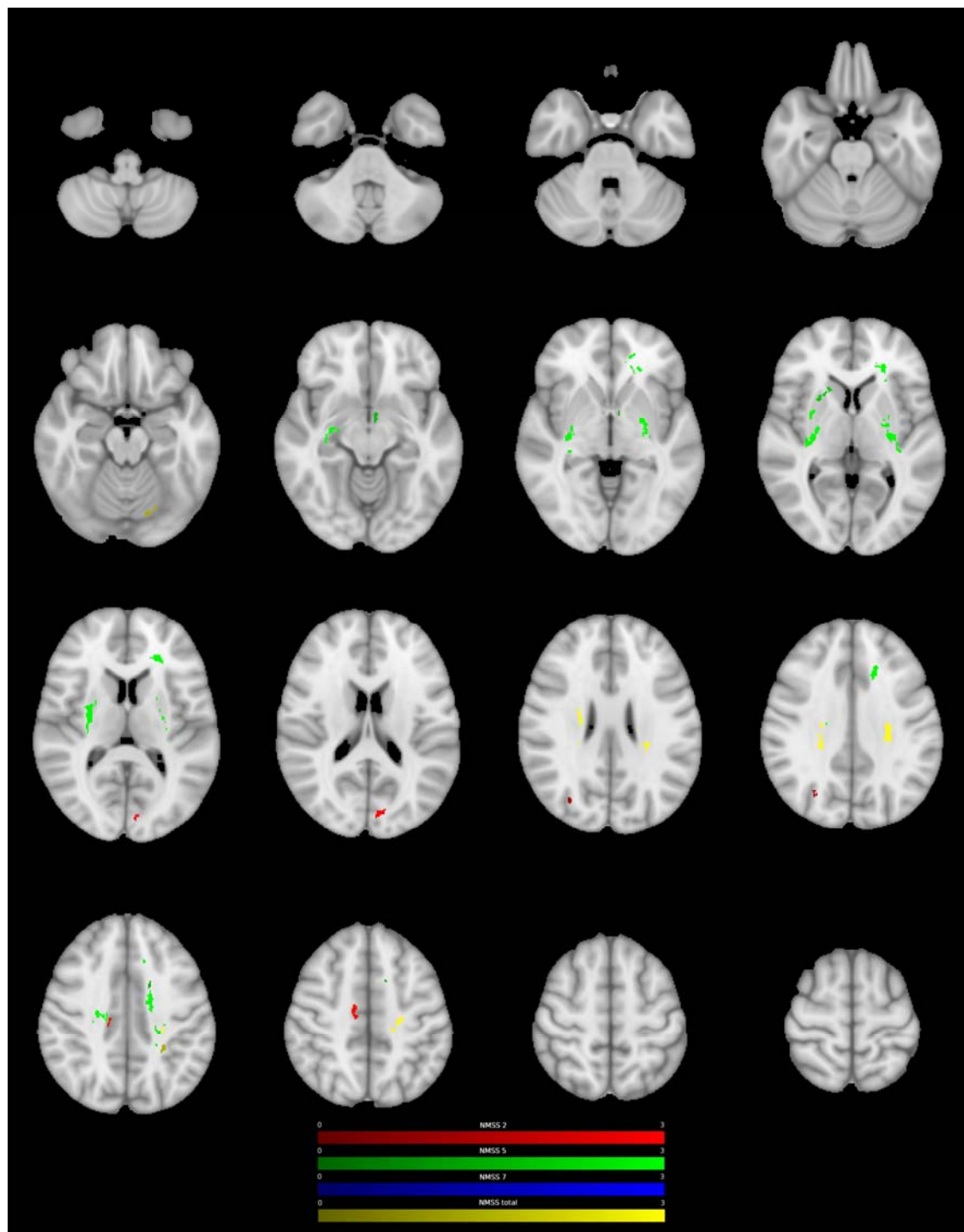


Figure 2. Clusters with a negative association between PD patients' ODI-values and postoperative change in NMSS-T (yellow), Domain 2 (sleep/fatigue, red), Domain 5

1 (attention/memory, green), and Domain 7 (urinary, blue), as revealed by the whole brain
2 analysis. P-Values were corrected for multiple comparisons using a permutation-based
3 approach.
4